—Technical Paper—

Interaction between Water/Hydrogen and Oxide Ceramics

Natsuko SAKAI,* Katsuhiko YAMAJI, Hideyuki NEGISHI, Teruhisa HORITA, Harumi YOKOKAWA, Yue Ping XIONG, and Michael B. PHILLIPPS

National Institute of Materials and Chemical Research (NIMC) (1-1 Higashi, Tsukuba, Ibaraki 305-8565, Japan)

Received November 19, 1999 ; Accepted February 17, 2000

A significant interaction was observed between water vapor and ionic or mixed conducting oxides as that found in proton conducting ceramics. For the case of yttrium substituted zirconium oxide (YSZ), the oxygen exchange on the surface is found to be governed by the interaction of water molecule and oxygen vacancy of YSZ in a humid atmosphere. This reaction rate was found to be much faster than the reaction between oxygen gas and vacancy, which was observed as very large values of rate constant for oxygen tracer exchange reaction on YSZ in $H_2{}^{18}O + {}^{18}O_2$ atmospheres at $T = 773$ K. The interfacial resistance of platinum electrode/YSZ electrolyte significantly decreased in humid atmospheres at $T = 761$ K.

Key Words : Water, YSZ, SIMS, Surface Reaction

1 Introduction

It has been well known that a significant interaction is observed between proton conducting ceramics such as $BaCe(Yb)O_{3-\alpha}$ and water vapor in ambient atmosphere. It is supposed that water molecule interacts with the oxygen vacancies in oxides as the following reaction:[1]

$$H_2O(g) + V_O^{\cdot\cdot} \leftrightarrow O_O^{\times} + 2\,H_i^{\cdot} \qquad (1)$$

The meaning of the symbols are listed above in the manuscript. Equation 1 indicates the dissolution of a water molecule is accompanied with the extinction of an oxygen vacancy ($V_O^{\cdot\cdot}$) and the formation of two interstitial protons ($H_i^{\cdot}$). The interstitial protons can migrate and act as the charge carriers instead of electronic holes.

Such as interactions between water and oxide ceramics have been discussed mainly about the cases of proton conducting oxides. However, the reaction (1) might be possible for other oxides having oxygen vacancies, although the amount of protons in the lattice is not large enough to govern the proton conduction. For example, Wagner *et al.*, has reported that the water solubility as interstitial proton is 2.1×10^{-5} mole per 1 mole of 17 wt. % Y_2O_3 substituted ZrO_2 (YSZ) at $T = 894$℃.[2] Recently, we have confirmed a significant interaction between rare earth substituted cerium oxide and water by secondary ion mass spectrometry (SIMS) technique:[3] A drastic increase was observed in the intensity of $^2D^-$ ion in $Ce_{0.8}M_{0.2}O_{1.9}$ (M = La, Nd, Sm, Gd, Yb, Y) after the annealing in 3% D_2O + 2% O_2 + 95% N_2 at $T = 880 \sim 990$℃ for 60 h, which indicates that the deuterium was absorbed in $Ce_{0.8}M_{0.2}O_{1.9}$. The solubility of hydrogen was determined as 8.5×10^{-3} mole fraction for $Ce_{0.8}Yb_{0.2}O_{1.9}$ at $T = 990$℃, which is 300 time higher than that in pure CeO_2 and one third of that in $SrCe_{0.95}Yb_{0.05}O_{3-\alpha}$.

The effect of such an interaction on the other electrical or physicochemical properties, for examples as proton conduction, has not confirmed yet. One objective of this paper is the investigation of the effect of water on the kinetics of the oxygen exchange reaction on YSZ surface, by using oxygen isotope (^{18}O) diffusion and SIMS analyses.

The exchange reaction between $^{18}O_2$ molecules and $^{16}O^{2-}$ ions in YSZ can be expressed by following processes;

$$1/2\,{}^{18}O_2(g) \rightleftarrows {}^{18}O_{ad} \qquad (2a)$$
$${}^{18}O_{ad} + V_O^{\cdot\cdot} \rightleftarrows {}^{18}O_O^{\times} + 2h^{\cdot} \qquad (2b)$$
$${}^{16}O_O^{\times} + 2h^{\cdot} \rightleftarrows {}^{16}O_{ad} + V_O^{\cdot\cdot} \qquad (2c)$$
$${}^{16}O_{ad} \rightleftarrows 1/2\,{}^{16}O_2(g) \qquad (2d)$$

The process (2a) represents the adsorption of $^{18}O_2$ molecule on YSZ surface, and (2b) is the reduction of an adsorbed oxygen atom ($^{18}O_{ad}$) by the interaction with an oxygen vacancy ($V_O^{\cdot\cdot}$) and electronic holes ($h^{\cdot}$) in YSZ. Since the $^{18}O^{2-}$ ion, which occupies the vacancy in the process (2b), diffuses fast into YSZ, the opposite reaction of (2b) are also governed by $^{16}O^{2-}$ ions as shown in (2c). As a result of combining all processes, the total reaction will be represented as:

$$1/2\,{}^{18}O_2(g) + {}^{16}O_O^{\times} \rightleftarrows {}^{18}O_O^{\times} + 1/2\,{}^{16}O_2(g) \qquad (2)$$

On the contrary, when $H_2{}^{18}O$ is used instead of $^{18}O_2$ as isotope source, the oxygen exchange reaction can be written as follows:

$$H_2{}^{18}O(g) \rightleftarrows H_2{}^{18}O_{ad} \qquad (3a)$$
$$H_2{}^{18}O_{ad} + V_O^{\cdot\cdot} \rightleftarrows 2H_i^{\cdot} + {}^{18}O_O^{\times} \qquad (3b)$$

The process (3b) is just the same as the reaction (1). However, since the solubility of water in YSZ is very small,[2] the opposite reaction proceeds as follows:

$$2H_i^{\cdot} + {}^{16}O_O^{\times} \rightleftarrows H_2{}^{16}O_{ad} + V_O^{\cdot\cdot} \quad (3c)$$

$$H_2{}^{16}O_{ad} \rightleftarrows H_2{}^{16}O(g) \quad (3d)$$

The total oxygen exchange reaction on YSZ surface via H_2O molecule will be expressed by incorporating the processes (3a)～(3d):

$$H_2{}^{18}O(g) + {}^{16}O_O^{\times} \rightleftarrows {}^{18}O_O^{\times} + H_2{}^{16}O(g) \quad (3)$$

It is expected that in humid atmosphere, the oxygen exchange reaction on YSZ surface may be governed by these two processes, *i.e.* (2) and (3). The main difference between (2) and (3) is the difference of carriers in charge transfer processes (b) and (c), where it is governed by electronic holes in YSZ for the process (2), and by the interstitial protons from dissolved H_2O for the process (3). It should be noted that the process (3) has seldom been considered for YSZ case, although water may often exist as impurity and dissolve into YSZ. This surface reaction is closely related to the cathode reaction in Solid oxide fuel cells (SOFCs), or oxygen permeation membranes. This paper also briefly reports the effect of water on the cathode reaction in the platinum electrode/YSZ electrolyte interface.

2 Experimental

2. 1 Oxygen tracer diffusion

YSZ single crystal (8 mol% Y_2O_3-ZrO_2, Earth Jewelry Co. Ltd., (100) plane oriented) was cut into small pieces with 3 mm × 3 mm × 1 mm, and the surface was cleaned by acetone. Pre-annealing was carried out in dry air or H_2O(21 hPa) + O_2 mixture in order to check the thermodynamic effect on the subsequent oxygen tracer exchange procedure, and the detailed conditions were shown in Table 1. The sample was then placed in a closed system, and the system was evacuated and then the stable isotopes of oxygen ($^{18}O_2$, ISOTEC Co. Ltd., 97% enriched) and/or water vapor ($H_2{}^{18}O$, 97% enriched) was introduced. The sample was rapidly heated to T = 773 K (500℃), held for 300 s, and then quenched to room temperature. Heating and cooling rate was around 40 K/s. The intensities of the mass spectra around M/e = 16 and M/e = 18 were collected by SIMS (CAMECA ims 5 f, primary ion: Cs^+, 10 kV, secondary ions: negative, −4.5 kV). It was confirmed that the mass signal around M/e = 18 corresponds to the $^{18}O^-$ ion, not to the other molecular ion, for example $H_2{}^{16}O^-$, by using high-resolution mass spectrometry ($M/\Delta M$ = 2800). Three types of analyses were adopted: Depth profiles were taken by etching the sample surface with a strong primary ion beam ($I(Cs^+)$ = 15～18 nA), and secondary ion images and line profiles were taken on the cross section of the sample with a focused, low energy beam ($I(Cs^+)$ = 10 pA). After collecting the depth profiles, the depth of etched area was measured by a surface profiler (Dektak^3, Veeco/Sloan Co. Ltd., USA). The depth profiles of ^{18}O relative concentration (C) in YSZ were then calculated from the intensities of $^{16}O^-$ and $^{18}O^-$ ions.

$$C(^{18}O \text{ concentration}) = I(^{18}O^-)/\{I(^{16}O^-) + I(^{18}O^-)\} \quad (4)$$

Table 1 Experimental conditions of pre-annealing and oxygen tracer exchange procedures.

Sample ID	Pre annealing				Oxygen tracer exchange			
	$p(O_2)$ /hPa	$p(H_2O)$ /hPa	T/K	t/h	$p(^{18}O_2)$ /hPa	$p(H_2{}^{18}O)$ /hPa	T/K	t/s
A	213	~0	773	3	24	22	773	300
B	213	~0	773	3	~0	21	773	300
C	25	25	773	87	25	21	773	300

2. 2 Electrochemical measurement

YSZ polycrystalline as an electrolyte was prepared by sintering TOSOH TS-8Y powder compact, which was shaped into a disk under a pressure 350 M Pa. The size of the sintered disk was *ca.* 17 mm diameter and 2 mm thick, and the relative density was above 99%. The surface of the disk was polished by using diamond paste. Platinum(Pt) paste was used as working and counter electrodes. A platinum wire was used as reference electrode, attached of the side wall of the YSZ disk. The working electrode was exposed to dry or humid air ($p(O_2) = 2.13 \times 10^2$ hPa). The partial pressure of water vapor was controlled by flowing air through H_2O trap, and it was kept at *ca.* 7.6 hPa in humid atmospheres. The reference and counter electrode was exposed to dry air. The flow rate was kept to 100 cm min^{-1}. AC impedance, approximately in open circuit condition, was measured by an impedance analyzer (SI 1260, Solatron), from 10 mHz to 1 MHz with 50 mV amplitude.

3 Results and Discussion

3. 1 Effect of water on oxygen tracer exchange and diffusion in YSZ

The symbols in Fig. 1 represent the depth profiles of ^{18}O relative concentration in YSZ single crystal annealed in different humid atmospheres as shown in Table 1. The ^{18}O concentration profiles were fitted to a diffusion equation solved by Crank[4] assuming a semi-infinite media and effect of surface reaction.

$$\frac{C - C_0}{C_g - C_0} = \mathrm{erfc}\frac{z}{2\sqrt{D_O^* t}} - \exp(bz + b^2 D_O^* t)\,\mathrm{erfc}\left\{\frac{z}{2\sqrt{D_O^* t}} + b\sqrt{D_O^* t}\right\} \quad (5)$$

$$\text{Where } b = k/D_O^* \quad (6)$$

Oxygen tracer diffusion coefficient (D_O^*) and surface reaction rate constant (k) were determined by the fitting where the other parameters were fixed at C_g = 0.97, C_0 = 0.002 (natural abundant of ^{18}O), t = 300 s. The results were summarized in Fig. 2.

Since the data shown in Fig. 1 are restricted in the vicinity of surfaces, the secondary ion images were taken for $^{18}O^-$ and $^{16}O^-$ ion on the cross section of sample A in order to obtain a full-length diffusion profile. The result is shown in Fig. 3(a), which indicates that oxygen tracer diffuse into *ca.* 10 μm in YSZ crystal. Fig. 3(b) shows a line profile of ^{18}O relative concentration on cross section, and it can also be fitted to eq. (5). It should be noted

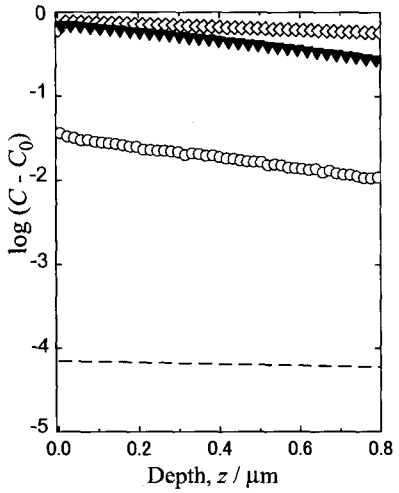

Fig. 1 Depth profile of normalized relative concentration of ^{18}O ($C - C_0$) in YSZ single crystal annealed at $T = 773$ K for 300 s: ◇; sample A, ▼; sample B; ○; sample C. Dotted line is the calculated depth profile by eq. (5) with D_O^* and k data in dry O_2 (1 atm = 1013 hPa) after Manning *et al.*[5]

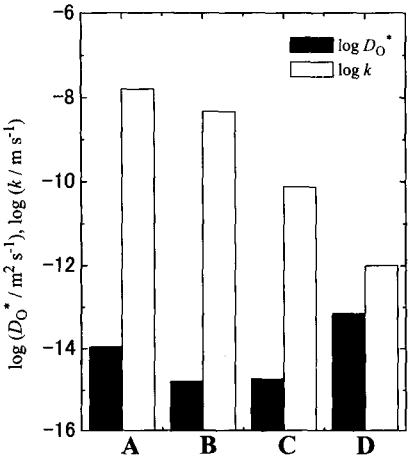

Fig. 2 Oxygen tracer diffusion coefficient (D_O^*) and surface reaction rate constant (k) at $T = 773$ K: A, B, C corresponds to the data of sample A, B, C in table 2 respectively. D; literature data obtained in dry O_2.[5]

that the ^{18}O relative concentration obtained in the line profile was lower than that in depth profiles. This is due to the adsorption of ^{16}O which comes from oxygen gas in the measuring chamber of SIMS, which was observed only in imaging and line scan analyses with low energy primary ion beam. This effect results in the relatively low surface reaction rate constant (k), but no significant changes in diffusion coefficient (D_O^*). The diffusion coefficients determined for sample A was 1.2×10^{-14} m^2 s^{-1} from depth profiles, and 1.1×10^{-14} m^2 s^{-1} for line profiles, which are in good agreement each other.

The oxygen tracer diffusion coefficients and surface reaction rate constants in YSZ have been measured in $p(^{18}O_2) = 1$ atm = 1013 hPa at various temperatures by Manning *et al.*,[5] and their results were compared with the present data in Figs. 1 and 2. Since they used a different annealing time for tracer diffusion, the ^{18}O concentration profile was estimated by eq. (5) with $t = 300$ s, and shown as dotted line in Fig. 1

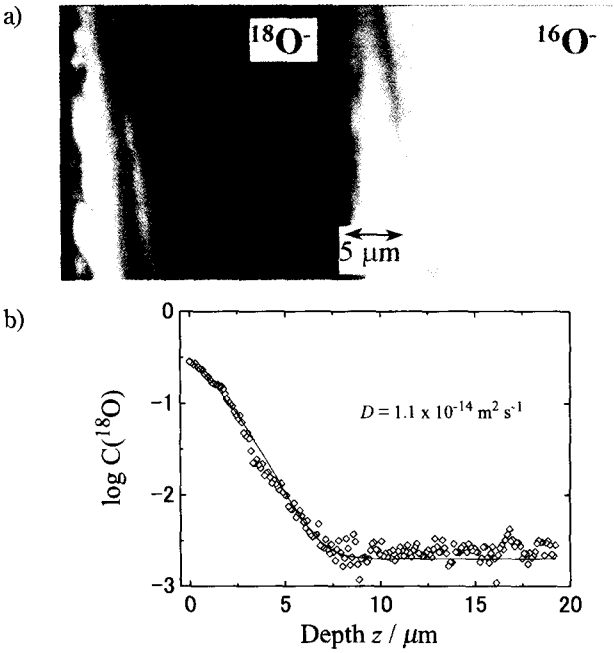

Fig. 3 Concentration profiles of oxygen tracer on the cross section of sample B: (a) SIMS secondary ion images for $^{18}O^-$ ion (left) and $^{16}O^-$ ion (right). (b) line profile of relative concentration of ^{18}O.

The present data indicate that remarkable high surface reaction rate constants (k) were obtained in humid atmospheres. However, the data greatly depend on the combination of experimental condition in pre-annealing and tracer diffusion. The k value of sample A was 10^4 times higher than the literature data obtained in dry O_2,[5] and sample C was 75 times. In Fig. 1, all present data exhibit very high relative concentration of ^{18}O, which is due to high surface reaction rate constants. On the contrary, the tracer diffusion coefficients (D_O^*) in humid atmospheres were founded to be smaller than the data in dry O_2.

Two reasons can be considered for such high reaction rate constants: one speculation is that the surface reaction on YSZ is governed mainly by the interaction of H_2O molecule and O^{2-} ion in YSZ according to the process (3 a)-(3d). The k value of sample B, which was annealed in $H_2{}^{18}O$ without oxygen gas, is very similar to that of sample A annealed in $O_2 + H_2{}^{18}O$. This fact confirms that the surface reaction is mainly governed by $H_2{}^{18}O$.

The other reason is the thermodynamic effect, which may be caused by the gradient of chemical potential of water between gas phase and YSZ. This effect concerns to the cases of samples A and B, those were pre-annealed in dry air. In such a pre-annealing condition, the activity of H_2O in YSZ is considered to be very low, much lower than that in subsequent tracer diffusion. Hence, the dissolution of $H_2{}^{18}O$ is enhanced according to the gradient of the activity between gas phase and YSZ in the vicinity of surface. To eliminate this effect, the pre-annealing should be carried out in the same atmosphere

as that in subsequent tracer exchange procedure. For sample C, the partial pressures of oxygen gas and water vapor were set as close as possible between pre-annealing and tracer exchange conditions. The obtained surface reaction rate constant of sample C was much smaller than those of samples A or B, however it was still 75 times larger than that obtained in dry O_2 by Manning *et al*. These results indicate that the tracer exchange reaction on YSZ is mainly governed by the interaction between water vapor and oxide ion in YSZ lattice, which is much faster than that between gaseous oxygen and oxide ion. It is considered that the solubility and mobility of interstitial protons ($H_i^{\cdot}$) are much larger than those of electronic holes ($h^{\cdot}$), which will cause a large difference in reaction rates.

It has still remained unclear why the diffusion coefficients decrease in humid atmosphere. The possibility of thermodynamic effect is denied because almost the same D_O^* values were obtained for samples B and C. According to eq. (1), the dissolution of a water molecule is accompanied with the generation of an interstitial proton and the extinction of an oxygen vacancy in YSZ. However, considering the water solubility in YSZ, the amount of extinguished vacancy is less than 0.1%, which hardly seems to affect on the diffusion kinetics. More experimental data such as effect of temperatures or water partial pressures should be required to investigate this effect, which is to be done in future works.

The literature data of D_O^* and k reported by Manning and his coworkers have been measured in dry O_2. Although there is no data of humidity in the system they used, the water vapor pressure in their system is expected to be very low because they obtained very small k values in a wide temperature range. However, they reported a curious temperature dependence of oxygen surface reaction rate constants both of YSZ and of $Ce_{0.9}Gd_{0.1}O_{2-x}$.[6] That is, the k values obtained at temperatures below 1073 K were slightly higher than those estimated from the temperature dependence above that temperature. As a result, two slopes were obtained for the Arrhenius plot of surface reaction rate constant, and lower activation energy was derived from the k values below 1073 K, whereas such a behavior was not observed for diffusion coefficients. A discontinuous change was observed in $b = k/D_O^*$ around $T = 1100 \sim 1200$ K. Their results indicate that the surface reaction kinetics was changed below and above that temperature range, which is hard to understand if only one diffusion kinetic is considered. It should be noted that both amounts of dissolved and adsorbed water will increase with decreasing temperature, so that it becomes more difficult to maintain a completely dry atmosphere. The effect of a trace amount of water in the system might be considered in such a condition.

3.2 Effect on the electrochemical property

Figure 4 shows the AC impedance spectra of YSZ polycrystalline at $T = 761$ K in dry and humid atmospheres. In the experiment, the impedance spectrum was collected first in dry air, and then the atmosphere of cathode side was changed to a humid atmosphere. The impedance spectra can be divided into two depressed semicircles. From the higher frequency, each real-axis intercept of the semicircles can be corresponded to (a) electrolyte and contact resistance and (b) electrode/electrolyte interfacial resistance. The obtained data clearly shows that the second semicircle becomes smaller and the interfacial resistance drastically decreased in humid atmosphere on cathode side, whereas electrolyte and contact resistances did not change significantly. When the atmosphere on cathode side was changed again from humid to dry atmosphere, the interfacial resistance increased again, however it took a long relaxation time.

Since the results were obtained in approximately open circuit condition, the effect of electric potential can be neglected. The present results are very preliminary and more detailed experiments will be required to check the reproducibility. However, the decrease of the interfacial resistance in humid atmosphere seems to be in good agreement with the changes of the surface reaction mechanism from the slow process with dry oxygen gas to the fast one with water vapor, which may decrease the reaction overpotential on the cathode.

4 Conclusion

The interaction of oxide ceramics and water vapor in ambient atmospheres was found for the oxygen exchange reaction on YSZ. The fast interaction of water vapor and oxide ion in YSZ plays a main role of oxygen exchange reaction in humid atmosphere. The concentration of water as interstitial proton is very low in YSZ, but is considered to be enough higher than that of electronic holes, which will be the reason of fast reaction rate.

The results of electrochemical measurement of YSZ with platinum electrodes indicated that the increase of humidity on cathode side significantly enhance the reaction at electrode/electrolyte interface and reduce the interfacial resistance. This effect should be investigated in future work more intensively from the viewpoints of utilizing this material for the electrolytes in electrochemical devices such as SOFCs or oxygen permeation membranes, in which the cathode reaction kinetics may control the efficiency or the performance of total systems.

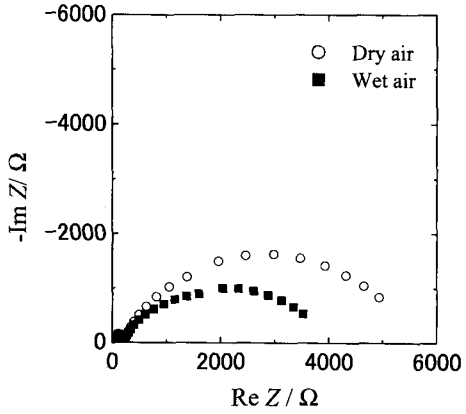

Fig. 4 Effect of atmospheres on complex impedance plots for YSZ polycrystalline with platinum electrodes at $T = 761$ K: □; dry air (100 ml min^{-1}) for both sides of YSZ, ■ cathode side: air + H_2O (7.6 hPa), anode side: dry air.

List of Symbols

T ; temperature, K
$V_O^{\cdot\cdot}$; an oxygen vacancy in the lattice
$O_O^{\times}$; an oxide ion (O^{2-}) in the lattice
$H_i^{\cdot}$; a proton (H^+) at interstitial site
O_{ad} ; an oxygen atom adsorbed on YSZ surface
$h^{\cdot}$; an electronic hole in the lattice
H_2O_{ad} ; a water molecule adsorbed on YSZ surface
M/e ; position of a signal in mass spectrum
I ; Ion current, A
C ; relative concentration of oxygen tracer (^{18}O)
p ; pressure, Pa
C_0 ; background relative concentration of oxygen tracer (^{18}O) in YSZ
C_g ; relative concentration of oxygen tracer (^{18}O) in gas phase
D_O^* ; oxygen tracer diffusion coefficient, $m^2\ s^{-1}$
k ; rate constant of surface reaction, $m\ s^{-1}$
t ; annealing time, s
z ; distance from the surface, m

References

1) Y. Larring and T. Norby, *Solid State Ionics*, **77**, 147 (1995).
2) C. Wagner, *Berichite der Bunsengesellschaft, Phys. Chem.*, **72**(7), 778 (1968).
3) N. Sakai, K. Yamaji, T. Horita, H. Yokokawa, Y. Hirata, S. Sameshima, Y. Nigara, and J. Mizusaki, *Solid State Ionics*, **125**, 325 (1999).
4) J. Crank, *Mathematics of Diffusion*, Oxford University Press, Oxford, UK (1975).
5) P. S. Manning, J. D. Sirman, R. A. De Souza, and J. A. Kilner, *Solid State Ionics*, **100**, 1 (1997).
6) P. S. Manning, J. D. Sirman, and J. A. Kilner, *Solid State Ionics*, **93** 125 (1997).